Adaptive-Neural-Network-Based Trajectory Tracking Control for a Nonholonomic Wheeled Mobile Robot With Velocity Constraints

Ziyu Chen , Yang Liu , Wei He , *Senior Member, IEEE*, Hong Qiao , *Fellow, IEEE*, and Haibo Ji

Abstract—In this article, an adaptive neural network control scheme is presented for an uncertain wheeled mobile robot (WMR) with velocity constraints and nonholonomic constraints. In practice, dynamic parameters of the system, which may change in some conditions, are hard to obtain precisely, and the velocity of the WMR should be constrained for safety. To deal with the uncertainty of the robot, adaptive neural networks are used to approximate unknown robotic dynamics, and the barrier Lyapunov function is used to guarantee the constraint on velocity. The tracking error of the closed-loop system is proven to converge to a small neighborhood of zero. Both simulation studies and practical experiments are provided to illustrate the effectiveness of the proposed control scheme.

Index Terms—Adaptive neural networks, barrier Lyapunov function (BLF), velocity constraint, wheeled mobile robot (WMR).

Ziyu Chen is with the Department of Automation, University of Science and Technology of China, Hefei 230027, China, and also with the State Key Laboratory of Management and Control for Complex Systems, Institute of Automation, Chinese Academy of Sciences, Bejing 100190, China (e-mail: ziyuchen@mail.ustc.edu.cn).

Haibo Ji is with the Department of Automation, University of Science and Technology of China, Hefei 230027, China (e-mail: jihb@ustc.edu.cn).

Yang Liu is with the Department of Mechanical Engineering, University of Science and Technology Beijing, Beijing 100083, China with the Beijing Key Laboratory of Research and Application for Robotic Intelligence of Hand-Eye-Brain Interaction, Beijing 100190, China, and also with the Cloud Computing Center, Chinese Academy of Sciences, Dongguan 523808, China (e-mail: b20180283@xs.ustb.edu.cn).

Wei He is with the Institute of Artificial Intelligence and the School of Automation and Electrical Engineering, University of Science and Technology Beijing, Beijing 100083, China (e-mail: weihe@ieee.org).

Hong Qiao is with the State Key Laboratory of Management and Control for Complex Systems, Institute of Automation, Chinese Academy of Sciences, Beijing 100190, China with the CAS Center for Excellence in Brain Science and Intelligence Technology, Shanghai 200031, China with the University of Chinese Academy of Sciences, Beijing 100049, China, and also with the University of Science and Technology of China, Hefei 230027, China (e-mail: hong.qiao@ia.ac.cn).

Color versions of one or more of the figures in this article are available online at http://ieeexplore.ieee.org.

Digital Object Identifier 10.1109/TIE.2020.2989711

I. INTRODUCTION

AS AN important branch of mobile robot [1]–[3], the wheeled mobile robot (WMR) has been deeply investigated and widely applied in many fields, such as service industry, industry, national defense industry, agriculture, etc. [4]–[6].

The WMR is a typical class of nonholonomic system [7], [8]. Based on the assumption that wheeled robots do not slip during movement, which is mathematically equivalent to a set of nonintegrable first-order differential constraints, nonholonomic constraints can be intuitively visualized in a situation where the mobile robot cannot experience lateral translations, and the velocity in that direction cannot be integrated [9]. In accordance with Brockett's theorem [10], nonholonomic systems cannot be stabilized merely through smooth time-invariant feedback control laws[11]. Thus, it is generally a challenging task to develop a proper controller to achieve stabilization and trajectory tracking of the nonholonomic WMR[12].

In WMR systems, speed of wheels and the maximum angular velocity are always limited due to safety consideration [13]. If the control strategy is designed without considering these constraints, the system would perform poorly and even incur instability[14]. Many efforts have been devoted to the control of mobile robots with velocity constraints. In [15], a sliding-mode control (SMC) scheme was proposed to stabilize a mobile robot while adhering to the physical constraints on its configuration variables. The design of controller gains was in accordance with the restrictions on the initial condition domain. In [16], a physical-limit-constrained minimum velocity norm coordinating scheme for a wheeled mobile redundant manipulator was proposed. Such a scheme can not only coordinate the mobile platform and the manipulator to fulfill the end-effector task with optimal index, but also consider the physical limits of the robot. However, in aforecited works, the system is considered with known parameters, which are almost impossible to be obtained precisely in practice. For example, it is very difficult to obtain friction and damping coefficients due to uncertainties of the pavement, and some system parameters are unknown because of the absence of detailed specification.

In recent years, the research of neural network (NN)-based tracking algorithms for the WMR with unknown system parameters has attracted attention from many scholars. NNs can approximate nonlinear functions with arbitrary precision under certain regions [17]–[20] and have been widely used to deal

with control problems of uncertain nonlinear systems [21]–[25]. Many efforts have been made to solve the tracking problem of the WMR with unknown system parameters. In [26], an NN approach for the tracking problem of mobile robots was proposed. Nonlinear approximation capabilities of NNs have been used to improve the control performances of classical kinematic feedback control schemes. In [27], an adaptive-NN-based tracking control algorithm was proposed for the WMR system with full state constraints. If system parameters are chosen properly, the proposed scheme can guarantee uniform ultimate boundedness for all signals in the WMR system, and the tracking error converges to a bounded compact set of zero.

However, only a few papers considered the dynamic WMR system with velocity constraints for position trajectory tracking based on NNs. The constraints for velocity need to be considered in the design of NN adaptive laws and Lyapunov functions, which will bring more challenges due to the effect of velocity constraints for NN adaptive laws. In [27], the system was considered with full state constraints, which come from the limitations for the forward speed of wheels and steering angular velocity. While the controller in [27] was designed to track the velocity trajectory, the decrement of position errors was not considered. When the initial position error is large, in order to reduce position errors, the auxiliary input velocity may be greater than constraint values. The control law in [27] cannot cope with this situation.

In this article, an adaptive-NN-based control scheme is proposed for an uncertain WMR system with nonholonomic constraints and velocity constraints. With the proposed method, the position errors can converge to a small neighborhood of zero, while the velocity constraints are not violated. The main contributions of this article are as follows.

1) An adaptive NN control scheme for an uncertain WMR system is designed to approximate uncertain or time-varying parameters. As a result, the robustness of the WMR system is improved effectively.

2) Velocity constraints are not violated with the proposed control. The barrier Lyapunov function is used to design the control law to prevent the violation of velocity constraints.

3) The proposed method can cope with the case that the auxiliary input velocity is greater than constraints.

The rest of this article is organized as follows. Section II gives preliminaries and dynamics of a WMR system. Controller designs are given in Sections III and IV. In Section V, the performance of the proposed control scheme is illustrated by simulations. Section VI provides experimental results. Finally, Section VII concludes this article.

II. PRELIMINARIES AND PROBLEM FORMULATION

A. Lemmas and Definitions

Definition 1: The operator $\otimes$ is defined as

$$x \otimes y = [x_1, x_2, ..., x_n]^T \otimes [y_1, y_2, ..., y_n]^T$$
$$= [x_1 y_1, x_2 y_2, ..., x_n y_n]^T \quad \forall x, y \in \mathbb{R}^n$$

where $x = [x_1, x_2, ..., x_n]^T$ and $y = [y_1, y_2, ..., y_n]^T$ are vectors.

Definition 2: The function $\text{sgn}(\cdot)$ is defined as

$$\text{sgn}(x) = \begin{cases} 1, & x > 0 \\ 0, & x = 0 \\ -1, & x < 0 \end{cases}.$$

B. Problem Formulation

Considering a three-degree-of-freedom WMR [28], [29]

$$M(q)\ddot{q} + C(q, \dot{q})\dot{q} + F(\dot{q}) = B(q)\tau + A(q)\lambda \quad (1)$$

where $q = [q_1, q_2, q_3]^T = [x, y, \theta]^T$ is the position vector, and $M(q) \in \mathbb{R}^{3 \times 3}$ is a symmetric positive-definite inertia matrix with the form of

$$M(q) = \text{diag}[m, m, I]^T \quad (2)$$

where m is the mass of the WMR, I is the moment of inertia of the WMR, $C(q, \dot{q}) \in \mathbb{R}^{3 \times 3}$ is the centripetal and Coriolis matrix, $B(q) \in \mathbb{R}^{3 \times 2}$ is the input transformation matrix, $\tau \in \mathbb{R}^{2 \times 1}$ is the torque input vector, $F(\dot{q}) \in \mathbb{R}^{3 \times 1}$ denotes the friction vector, and $A(q)\lambda \in \mathbb{R}^{3 \times 1}$ is the nonholonomic constraint force.

The nonholonomic constraint of the robot is

$$\dot{x} \cos(\theta) + \dot{y} \sin(\theta) = 0. \quad (3)$$

Nonholonomic constraints can be written as $A(q)\dot{q} = 0$. $H(q)$ is formed by a set of smooth and linearly independent vector fields spanning the null space of $A(q)$, i.e., $H^T(q)A(q) = 0$. Then, (1) can be reformed as

$$\dot{q} = H(q)v$$
$$M_1(q)\dot{v} + C_1(q, \dot{q})v + F_1(q, \dot{q}) = B_1(q)\tau \quad (4)$$

where $M_1(q) = H^T(q)M(q)H(q)$, $C_1(q, \dot{q}) = H^T(q) [M(q)\dot{H}(q) + C(q, \dot{q})H(q)]$, $F_1(q, \dot{q}) = H^T(q)F(\dot{q})$, and $B_1(q) = H^T(q)B(q)$.

Choose

$$H(q) = \begin{bmatrix} -\sin(\theta) & \cos(\theta) & 0 \\ 0 & 0 & 1 \end{bmatrix}^T. \quad (5)$$

Then, we have

$$v = [v_1 \ v_2]^T = [v_1 \ w]^T \quad (6)$$

where v_1 and w are the linear and angular velocities, respectively. For $H(q)$, one has $C_1 = 0$ and $M_1 = \text{diag}[M_{111}, M_{122}]^T = \text{diag}[m, I]^T$. M_1 is a constant diagonal matrix. Velocity constraints are $|v_i| < v_{u1i}, i = 1, 2$, and $v_{u1} = [v_{u11}, v_{u12}]^T$. Similar to [30], the following auxiliary velocity input ensures that the position tracking errors of q are asymptotically stable:

$$v_{c0} = \begin{bmatrix} v_{c01} \\ v_{c02} \end{bmatrix} = \begin{bmatrix} v_{1d} \cos e_3 + k_1 e_1 \\ v_{2d} + k_2 v_{1d} e_2 + k_3 \sin e_3 \end{bmatrix} \quad (7)$$

where k_1, k_2, and k_3 are positive constants with $k_2 \geq 1$. v_{1d} and v_{2d} are desired velocity with $0 < v_{1d\min} < v_{1d} < v_{1d\max} <$

v_{u11}. The tracking errors are defined as

$$e = \begin{bmatrix} e_1 \\ e_2 \\ e_3 \end{bmatrix}^T = \begin{bmatrix} -\sin(\theta) & \cos(\theta) & 0 \\ -\cos(\theta) & -\sin(\theta) & 0 \\ 0 & 0 & 1 \end{bmatrix}^T (q_d - q). \quad (8)$$

The control objective is to design an adaptive NN control scheme such that the WMR can track the desired position trajectory while velocity constraints are not violated.

III. MODEL-BASED CONTROL

A. Design of Model-Based Control

We propose the model-based control law as

$$\tau = B_1^{-1} \left\{ M_1 \left\{ \begin{bmatrix} A_1' \\ A_2' \end{bmatrix} \otimes \left(-\rho \begin{bmatrix} V_{11} \\ V_{12} \end{bmatrix} + (v - v_{c1}) \otimes \dot{v}_{c0} \right) \right\} + F_1 \right\} \quad (9)$$

where ρ is a positive constant and $A_i' = \begin{cases} \frac{1}{A_i}, & A_i \neq 0 \\ 0, & A_i = 0 \end{cases}$, $i = 1, 2$; $A = [A_1, A_2]^T$ is defined as

$$A = v - v_{c0} + \left[\frac{\text{sgn}(v_1) h_1(v_1)}{v_{u11} - |v_1|}, \frac{\text{sgn}(v_2) h_2(v_2)}{v_{u12} - |v_2|} \right]^T \quad (10)$$

where $h_i(x)$, $i = 1, 2$, are defined as

$$h_i(x) = \begin{cases} 1, & |x| > v_{u2i} \\ 0, & \text{others} \end{cases}. \quad (11)$$

V_1 is the value of the Lyapunov function, and $V_1 = V_{11} + V_{12}$. The Lyapunov function is chosen as

$$V_1 = \frac{1}{2} z^T z + f(v) + g(v_{c0}) \quad (12)$$

where

$$z = [z_1, z_2]^T = v - v_{c0} \quad (13)$$

$$f(v) = f_1(v) + f_2(v) \quad (14)$$

$$f_i(v) = \begin{cases} -\ln \frac{v_{u1i} - |v_i|}{v_{u1i} - v_{u2i}}, & |v_i| > v_{u2i} \\ 0, & \text{others} \end{cases} \quad (15)$$

$$g(v_{c0}) = -\left\{ \frac{1}{2} (v_{c1} - v_{c0})^T (v_{c1} - v_{c0}) + f(v_{c1}) \right\} \quad (16)$$

where $v_{u2} = [v_{u21}, v_{u22}]^T$ is a positive constant matrix and $0 < v_{u2i} < v_{u1i}$. v_{c1} is the minimum point of $\{ \frac{1}{2} z^T z + f(v) \}$ and is written as

$$v_{c1} = [v_{c11}, v_{c12}]^T \quad (17)$$

$$v_{c1i} = \begin{cases} \text{sgn}(v_{c0i}) C_{v_{c1}}, & |v_{c0i}| > v_{u2i} + \frac{1}{v_{u1i} - v_{u2i}} \\ \text{sgn}(v_{c0i}) v_{u2i}, & v_{u2i} < |v_{c0i}| \leq v_{u2i} + \frac{1}{v_{u1i} - v_{u2i}} \\ v_{c0i}, & |v_{c0i}| \leq v_{u2i} \end{cases} \quad (18)$$

for $i = 1, 2$, where $C_{v_{c1}} = \frac{|v_{c0i}| + v_{u1i} - \sqrt{(|v_{c0i}| - v_{u1i})^2 + 4}}{2}$.

V_1 is a continuous positive function when the velocity meets the constraint, because $f(v)$ is continuous, $g(v_{c0})$ is a continuous

function independently of v, and $-g(v_{c0})$ equals the minimum of $\frac{1}{2} z^T z + f(v)$. For $|v_i| < v_{u1i}$, $i = 1, 2$, if $v_i \to v_{u1i}$, it has $V_1 \to \infty$, so the Lyapunov function (12) can help design controller that can constrain velocities.

Note that barrier Lyapunov functions in other WMR control methods require that the desired values cannot exceed constraints. However, in this article, the desired values of the barrier Lyapunov function are auxiliary velocity input, which may exceed the constraints when the WMR is far away from the desired position. Therefore, the Lyapunov function (12) is designed, which can deal with this situation. Equation (12) can be divided into three parts: $\frac{1}{2} z^T z$ is used for decreasing $\|v - v_{c0}\|$, $f(v)$ is used to constrain the velocity, and $g(v_{c0})$ is used to ensure that the minimum value of V_1 is 0.

V_1 can be divided into two parts, which correspond to v_1 and v_2, as follows:

$$V_1 = V_{11} + V_{12} \quad (19)$$

where

$$V_{1i} = \frac{1}{2} (v_i - v_{c0i})^2 + f_i(v_i) - \frac{1}{2} (v_{c1i} - v_{c0i})^2 - f_i(v_{c1i}). \quad (20)$$

B. Stability Analysis of the Model-Based Control Law

Theorem 1: For the system described by (1), with the control law (9), for initial states satisfying the constraints $|v_i| < v_{u1i}$, $i = 1, 2$, the states of the system would not violate the constraints. When $|v_{c0i}| < v_{u2i}$, $i = 1, 2$, velocity error signals z and position error signals e would converge to zero. The closed-loop control system is asymptotically stable.

Proof: Differentiating V_1 with respect to time yields

$$\dot{V}_1 = z \dot{z} + f'(v) + g'(v_{c0}) \quad (21)$$

where

$$f'(v) = \sum_{i=1}^{2} \begin{cases} \frac{\text{sgn}(v_i)}{v_{u1i} - |v_i|} \dot{v}_i, & |v_i| > v_{u2i} \\ 0, & \text{others} \end{cases} \quad (22)$$

$$\begin{aligned} g'(v_{c0}) &= \{ -z \dot{z} - f'(v) \} |_{v=v_{c1}} \\ &= -(v_{c1} - v_{c0})^T (\dot{v}_{c1} - \dot{v}_{c0}) \\ &\quad - \sum_{i=1}^{2} \begin{cases} \frac{\text{sgn}(v_{c1i}) \dot{v}_{c1i}}{v_{u1i} - |v_{c1i}|}, & |v_{c1i}| > v_{u2i} \\ 0, & \text{others} \end{cases}. \end{aligned} \quad (23)$$

In order to simplify (23), classify v_{c0i} into the following three conditions.

1) If $|v_{c0i}| \leq v_{u2i}$, then $v_{c1i} = v_{c0i}$ and $(v_{c1i} - v_{c0i}) \dot{v}_{c1} = 0$.
2) If $|v_{u0i}| < |v_{c0i}| \leq v_{u2i} + \frac{1}{v_{u1i} - v_{u2i}}$, then v_{c1i} is constant and $\dot{v}_{c1} = 0$.
3) If $|v_{c0i}| > v_{u2i} + \frac{1}{v_{u1i} - v_{u2i}}$, then $v_{u2i} < |v_{c1i}| < v_{u1i}$; then, $\frac{1}{2} (v_i - v_{c0i})$ and $f_i(v)$ are both smooth at $v_i = v_{c1i}$. As v_{c1} is the minimum point of $\{ \frac{1}{2} z^T z + f(v) \}$, we have $\frac{\partial \{ \frac{1}{2} z^T z + f(v) \}}{\partial v_i} |_{v_i = v_{c1i}} = v_{c1i} - v_{c0i} + \frac{\text{sgn}(v_{c1i})}{v_{u1i} - |v_{c1i}|} = 0$.

Finally, for any $v_{c0i} \in \mathbb{R}, i = 1, 2$, we have

$$(v_{c1} - v_0)^T \dot{v}_{c1} + \sum_{i=1}^{2} \begin{cases} \frac{\text{sgn}(v_{c1i})\dot{v}_{c1i}}{v_{u1i} - |v_{c1i}|}, & |v_{c1i}| > v_{u2i} \\ 0, & \text{others} \end{cases} = 0. \tag{24}$$

Then, substituting (24) into (23), we obtain

$$g'(v_{c0}) = -(v_{c1} - v_{c0})^T \dot{v}_{c0}. \tag{25}$$

Substituting (10), (22), and (25) into (21) yields

$$\dot{V}_1 = A^T \dot{v} - (v - v_{c1})^T \dot{v}_{c0}. \tag{26}$$

Dividing $\dot{V}_1$ into two parts corresponding to v_1 and v_2, we obtain

$$\dot{V}_1 = \dot{V}_{11} + \dot{V}_{12} \tag{27}$$

$$\begin{bmatrix} \dot{V}_{11} \\ \dot{V}_{12} \end{bmatrix} = A \otimes \dot{v} - (v - v_{c1}) \otimes \dot{v}_{c0}. \tag{28}$$

Substituting (4) and (9) into (28) yields

$$\begin{bmatrix} \dot{V}_{11} \\ \dot{V}_{12} \end{bmatrix} = \rho \begin{bmatrix} V_{11} \\ V_{12} \end{bmatrix}. \tag{29}$$

Substituting (19) and (29) into (27) yields

$$\dot{V}_1 = -\rho V_1. \tag{30}$$

According to the above Lyapunov function, we can conclude that V_1 can converge to zero. When $|v_{c0i}| < v_{u2i}, i = 1, 2$, one has $v_{c1} = v_{c0}$ and $V_1 = \frac{1}{2} z^T z$. Therefore, z can converge to zero.

To further prove the convergence of position errors e, we rewrite the Lyapunov function in [30] as

$$V_2 = \frac{1}{2}(e_1^2 + e_2^2) + (1 - \cos e_3)/k_2 \tag{31}$$

$$\dot{V}_2 = \dot{e}_1 e_1 + \dot{e}_2 e_2 + \dot{e}_3 \sin e_3 / k_2 \tag{32}$$

where

$$\dot{e}_1 = e_2 v_2 - v_1 + v_{1d} \cos e_3 \tag{33}$$

$$\dot{e}_2 = -e_1 v_2 + v_{1d} \sin e_3 \tag{34}$$

$$\dot{e}_3 = v_{2d} - v_2. \tag{35}$$

Substituting (33)–(35) into (32) yields

$$\dot{V}_2 = (-v_1 + v_{1d} \cos e_3) e_1$$

$$+ v_{1d} \sin e_3 e_2 + \frac{(v_{2d} - v_2) \sin e_3}{k_2}. \tag{36}$$

Substituting (7) and (13) into (36) yields

$$\dot{V}_2 = -k_1 e_1^2 - z_1 e_1 - \frac{k_3 \sin e_3^2}{k_2} - \frac{z_2 \sin e_3}{k_2} \tag{37}$$

$$= -k_1 \left(e_1 + \frac{z_1}{2k_1}\right)^2 - \frac{k_3}{k_2}\left(\sin e_3 + \frac{z_2}{2k_3}\right)^2 + \frac{z_1^2}{4k_1} + \frac{z_2^2}{4k_2 k_3}. \tag{38}$$

For the convergence of z, we have that for any $\varepsilon_0 > 0$, there exists T_z; when $t > T_z$, we have $\|z\| < \varepsilon_0$. Therefore, when

$t > T_z$, we have

$$\dot{V}_2 \leq -k_1 \left(e_1 + \frac{z_1}{2k_1}\right)^2 - \frac{k_3}{k_2}\left(\sin e_3 + \frac{z_2}{2k_3}\right)^2 + \varepsilon_1 \tag{39}$$

where $\varepsilon_1 = \frac{\varepsilon_0^2}{4k_1} + \frac{\varepsilon_0^2}{4k_2 k_3}$. From (39), we can know that when $|e_1| > \sqrt{\frac{1}{k_1}\varepsilon_1} + \frac{\varepsilon_0}{2k_1}$ or $|\sin e_3| > \sqrt{\frac{k_2}{k_3}\varepsilon_1} + \frac{\varepsilon_0}{2k_3}$, $\dot{V}_2 < 0$. Because ε_0 can be arbitrary small, we can choose proper ε_0 satisfying $\sqrt{\frac{k_2}{k_3}\varepsilon_1} + \frac{\varepsilon_0}{2k_3} < \frac{\pi}{4}$. If $|e_3| > 2(\sqrt{\frac{k_2}{k_3}\varepsilon_1} + \frac{\varepsilon_0}{2k_3})$, then $|\sin e_3| > \sin 2(\sqrt{\frac{k_2}{k_3}\varepsilon_1} + \frac{\varepsilon_0}{2k_3}) > \sqrt{\frac{k_2}{k_3}\varepsilon_1} + \frac{\varepsilon_0}{2k_3}$ and $\dot{V}_2 < 0$. Therefore, when $\|e\| > (\sqrt{\frac{1}{k_1}\varepsilon_1} + \frac{\varepsilon_0}{2k_1}) + 2(\sqrt{\frac{k_2}{k_3}\varepsilon_1} + \frac{\varepsilon_0}{2k_3}) + l\{(\sqrt{\frac{1}{k_1}\varepsilon_1} + \frac{\varepsilon_0}{2k_1}) + 2(\sqrt{\frac{k_2}{k_3}\varepsilon_1} + \frac{\varepsilon_0}{2k_3})\}$, where l is the minimum value that satisfies $l > 5$, $\frac{10}{lk_2 v_{1dmin}} < 0.2$, $\frac{k_3}{2k_2 l^2} < 0.5$, $\frac{k_3}{k_2 v_{1dmin} l} < 0.1$, $1.1 v_{2max} \frac{10}{lk_2 v_{1dmin}} + v_{1dmax}(\frac{1}{l} + \frac{11 v_{1dmax}}{lv_{1dmin}} + \frac{k_3}{5l})\frac{10}{k_2 v_{1dmin}} < 0.2$, and $\frac{k_3}{lk_2 v_{1dmin}}(1 + 1.1 k_2 v_{1dmax} \frac{10}{v_{1dmin}} + \frac{k_3}{5}) < 0.2$, we have the following two conditions.

1) If $|e_1| > \sqrt{\frac{1}{k_1}\varepsilon_1} + \frac{\varepsilon_0}{2k_1}$ or $|e_3| > 2(\sqrt{\frac{k_2}{k_3}\varepsilon_1} + \frac{\varepsilon_0}{2k_3})$, then $\dot{V}_2 < 0$.

2) If $|e_1| < \sqrt{\frac{1}{k_1}\varepsilon_1} + \frac{\varepsilon_0}{2k_1}$ and $|e_3| < 2(\sqrt{\frac{k_2}{k_3}\varepsilon_1} + \frac{\varepsilon_0}{2k_3})$, then $|e_2| > l\{(\sqrt{\frac{1}{k_1}\varepsilon_1} + \frac{\varepsilon_0}{2k_1}) + 2(\sqrt{\frac{k_2}{k_3}\varepsilon_1} + \frac{\varepsilon_0}{2k_3})\}$, $|e_2| > \frac{l\varepsilon_0}{k_3} > \frac{l|z_2|}{k_3}$, $|e_2| > l|e_1|$, and $|e_2| > l|e_3|$.

For condition 2, setting the time of $|e_1| < \sqrt{\frac{1}{k_1}\varepsilon_1} + \frac{\varepsilon_0}{2k_1}$ and $|e_3| < 2(\sqrt{\frac{k_2}{k_3}\varepsilon_1} + \frac{\varepsilon_0}{2k_3})$ as t_0, we obtain $|e_{2(t=t_0)}| > \frac{l|z_2|}{k_3}$. Let $T = \frac{10}{lk_2 v_{1dmin}} < 0.2$. In order to analyze the mean value of $\dot{V}_2$ for $t_0 < t < t_0 + T$, we need to analyze the variation range of e_1, e_2, and e_3. From $|e_2| < l|e_1|$, $|e_2| > l|e_3|$, and (31), we obtain

$$V_{2(t=t0)} = \frac{1}{2}(e_{1(t=t0)}^2 + e_{2(t=t0)}^2) + \frac{(1 - \cos e_{3(t=t0)})}{k_2}$$

$$< \left(\frac{k_2 + 1}{2k_2 l^2} + \frac{1}{2}\right) e_{2(t=t0)}^2. \tag{40}$$

.

For $|e_{2(t=t0)}| > 2l\sqrt{\frac{k_2}{k_3}\varepsilon_1}$, we have $\dot{V}_2 < \varepsilon_1 < \frac{k_3}{4l^2 k_2} e_{2(t=t0)}^2 < \frac{k_3}{2l^2 k_2} V_{2(t=t0)}$. In the time between $t_0 < t < t_0 + T$, we have

$$V_2 = V_{2(t=t0)} + \int_{t_0}^{t} \dot{V}_2 dt. \tag{41}$$

Substituting $\dot{V}_2 < \frac{k_3}{2l^2 k_2} V_{2(t=t0)}$, $\frac{k_3}{2l^2 k_2} < 0.5$, $T < 0.2$, (40), $k_2 \geq 1$, and $l > 5$ into (41), we obtain

$$V_2 < V_{2(t=t0)} + \frac{k_3}{2l^2 k_2} V_{2(t=t0)} T < 1.1 V_{2(t=t0)}$$

$$< 1.1 \left(\frac{k_2 + 1}{2k_2 l^2} + \frac{1}{2}\right) e_{2(t=t0)}^2 < 0.594 e_{2(t=t0)}^2. \tag{42}$$

Substituting (42) into (31) yields

$$|e_2| < \sqrt{2V_2} < \sqrt{2 \times 0.594 e_{2(t=t0)}^2} < 1.1|e_{2(t=t_0)}| \quad (43)$$

$$|e_1| < \sqrt{2V_2} < 1.1|e_{2(t=t_0)}|. \quad (44)$$

For $\dot{e}_3 = -k_2 v_{1d} e_2 - k_3 \sin e_3 + z_2$, we have

$$e_3 = e_{3(t=t_0)} + \int_{t_0}^{t} (-k_2 v_{1d} e_2 - k_3 \sin e_3 + z_2) dt. \quad (45)$$

For the term $-k_3 \sin e_3$ in $\dot{e}_3$ that will decrease the absolute value of e_3, we have

$$|e_3| < |e_{3(t=t_0)}| + \int_{t_0}^{t} |-k_2 v_{1d} e_2 + z_2| dt. \quad (46)$$

Substituting (43), $|e_{2(t=t_0)}| > \frac{l|z_2|}{k_3}$, and $T < 0.2$ into (46), we obtain

$$|e_3| < |e_{3(t=t_0)}| + k_2 v_{1d\max} e_{2\max} T + |z_2| T$$

$$< |e_{3(t=t_0)}| + 1.1 k_2 v_{1d\max} |e_{2(t=t_0)}| T + \frac{k_3 |e_{2(t=t_0)}|}{l} T$$

$$< \frac{|e_{2(t=t_0)}|}{l} + \frac{11 v_{1d\max} |e_{2(t=t_0)}|}{l v_{1d\min}} + \frac{k_3 |e_{2(t=t_0)}|}{5l} \quad (47)$$

for

$$|e_2| > |e_{2(t=t_0)}| - |\dot{e}_2|_{\max} T$$

$$> |e_{2(t=t_0)}| - (|e_1|_{\max} |v_2|_{\max} + v_{1d\max} |e_3|_{\max}) T. \quad (48)$$

Substituting (47), $T = \frac{10}{l k_2 v_{1d\min}}$, and $1.1 v_{2\max} \frac{10}{l k_2 v_{1d\min}} + v_{1d\max}(\frac{1}{l} + \frac{11 v_{1d\max}}{l v_{1d\min}} + \frac{k_3}{5l}) \frac{10}{l k_2 v_{1d\min}} < 0.2$ into (48), we obtain

$$|e_2| > |e_{2(t=t_0)}| - \left\{ 1.1|e_{2(t=t_0)}| v_{2\max} T + v_{1d\max} \left(\frac{1}{l} |e_{2(t=t_0)}| \right. \right.$$

$$\left. \left. + \frac{11 v_{1d\max} |e_{2(t=t_0)}|}{l v_{1d\min}} + \frac{k_3 |e_{2(t=t_0)}|}{5l} \right) T \right\}$$

$$> |e_{2(t=t_0)}| - 0.2|e_{2(t=t_0)}| = 0.8|e_{2(t=t_0)}|. \quad (49)$$

If $e_2 > 0$, then

$$\dot{e}_3 = -k_2 v_{1d} e_2 - k_3 \sin e_3 + z_2$$

$$< -0.8 k_2 v_{1d} |e_{2(t=t_0)}| + k_3 (|\sin e_3| + \frac{|e_{2(t=t_0)}|}{l}). \quad (50)$$

For $\frac{k_3}{k_2 v_{1d\min} l} < 0.1$, we have

$$\dot{e}_3 < -0.7 k_2 v_{1d\min} |e_{2(t=t_0)}| + k_3 |\sin e_3|$$

$$< -k_2 v_{1d\min} \left(0.7|e_{2(t=t_0)}| - \frac{k_3 |e_{2(t=t_0)}|}{k_2 v_{1d\min} l} \left(1 \right. \right.$$

$$\left. \left. + 1.1 k_2 v_{1d\max} \frac{10}{v_{1d\min}} + \frac{k_3}{5} \right) \right)$$

$$< -k_2 v_{1d\min} |e_{2(t=t_0)}| (0.7 - 0.2) < 0. \quad (51)$$

Then, for $t_0 < t < t_0 + \frac{3}{5}T$, from (39), we have

$$\dot{V}_2 < \varepsilon_1. \quad (52)$$

For $t_0 + \frac{3}{5}T < t < t_0 + T$, we have

$$e_3 < e_{3(t=t_0+\frac{3}{5}T)} = e_{3(t=t_0)} + \int_{t_0}^{t_0+\frac{3}{5}T} \dot{e}_3$$

$$< e_{3(t=t_0)} - 0.5 k_2 v_{1d\min} |e_{2(t=t_0)}| \frac{3}{5} \frac{10}{l k_2 v_{1d\min}}$$

$$< e_{3(t=t_0)} - \frac{3}{l} |e_{2(t=t_0)}| < -\frac{2}{l} |e_{2(t=t_0)}|$$

$$< -4 \left(\sqrt{\frac{k_2}{k_3} \varepsilon_1} + \frac{|z_2|}{2k_3} \right). \quad (53)$$

Similarly, if $e_2 < 0$, for $t_0 + \frac{3}{5}T < t < t_0 + T$, we have

$$e_3 > 4 \left(\sqrt{\frac{k_2}{k_3} \varepsilon_1} + \frac{|z_2|}{2k_3} \right). \quad (54)$$

Therefore, we have

$$\dot{V}_2 < -\frac{k_3}{k_2} \left(\sin e_3 + \frac{z_2}{2k_3} \right)^2 + \varepsilon_1 < -3\varepsilon_1 \quad (55)$$

and

$$\int_{t_0}^{t_0+T} \dot{V}_2 = \int_{t_0}^{t_0+\frac{3}{5}T} \dot{V}_2 + \int_{t_0+\frac{3}{5}T}^{t_0+T} \dot{V}_2$$

$$< \frac{3}{5} T \varepsilon_1 - \frac{2}{5} T 3 \varepsilon_1 = -\frac{3}{5} T \varepsilon_1. \quad (56)$$

Therefore, we can obtain that for $t_0 < t < t_0 + T$, the mean value of $\dot{V}_2$ is less than $-\frac{3}{5}\varepsilon_1$ and $\dot{V}_2$ is less than ε_1.

Finally, we have that if $\|e\| > (\sqrt{\frac{1}{k_1} \varepsilon_1} + \frac{\varepsilon_0}{2k_1}) + 2(\sqrt{\frac{k_2}{k_3} \varepsilon_1} + \frac{\varepsilon_0}{2k_3}) + l\{(\sqrt{\frac{1}{k_1} \varepsilon_1} + \frac{\varepsilon_0}{2k_1}) + 2(\sqrt{\frac{k_2}{k_3} \varepsilon_1} + \frac{\varepsilon_0}{2k_3})\}$, then:

1) If $|e_1| > \sqrt{\frac{1}{k_1} \varepsilon_1} + \frac{\varepsilon_0}{2k_1}$ or $|e_3| > 2(\sqrt{\frac{k_2}{k_3} \varepsilon_1} + \frac{\varepsilon_0}{2k_3})$, then $\dot{V}_2 < 0$.

2) If $|e_1| < \sqrt{\frac{1}{k_1} \varepsilon_1} + \frac{\varepsilon_0}{2k_1}$ and $|e_3| < 2(\sqrt{\frac{k_2}{k_3} \varepsilon_1} + \frac{\varepsilon_0}{2k_3})$, in the following period of time T, $\overline{\dot{V}_2} < 0$ and $\dot{V}_2 < \varepsilon_1$.

Therefore, e will converge to $\Omega_1 := \{e \in \mathbb{R}^3 | \|e\| < (\sqrt{\frac{1}{k_1} \varepsilon_1} + \frac{\varepsilon_0}{2k_1}) + 2(\sqrt{\frac{k_2}{k_3} \varepsilon_1} + \frac{\varepsilon_0}{2k_3}) + l\{(\sqrt{\frac{1}{k_1} \varepsilon_1} + \frac{\varepsilon_0}{2k_1}) + 2(\sqrt{\frac{k_2}{k_3} \varepsilon_1} + \frac{\varepsilon_0}{2k_3})\}\}$. For $t \to +\infty$, we have $z \to 0$, $\varepsilon_0 \to 0$, and $\varepsilon_1 \to 0$. Thus, we have $e \to 0$. Therefore, the closed-loop control system is asymptotically stable.

IV. ADAPTIVE NN CONTROL

A. Design of the Adaptive NN Control Law

We propose the adaptive NN control law as

$$\tau = -\rho_1 B_1^{-1} \left(\begin{bmatrix} A_1' \\ A_2' \end{bmatrix} \otimes \begin{bmatrix} V_{11} \\ V_{12} \end{bmatrix} \right)$$

$$+ B_1^{-1} \left\{ \begin{bmatrix} A_1' \\ A_2' \end{bmatrix} \otimes (v - v_{c1}) \otimes (\hat{W}^T S(Z)) \right\} \quad (57)$$

where ρ_1 is the control gain, $\hat{W}^T S(Z)$ is the NN, $S(Z) = [S_1(Z), S_2(Z)]$, $S_i(Z) = [S_{i1}(Z), S_{i2}(Z), ..., S_{in}(Z)]^T$, $n =$
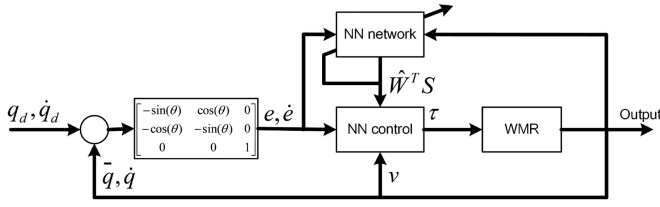
Fig. 1.   Block diagram of the proposed controller.

64 is the basis function of the RBF NN with $Z = [\dot{v}_{c0}^T, \frac{A_1}{(v_1 - v_{c11})}, \frac{A_2}{(v_2 - v_{c12})}, v^T]^T$, and $S_i(Z)$ are Gaussian functions. $\hat{W} = [\hat{W}_1, \hat{W}_2]$, $\hat{W}_i = [\hat{W}_{i1}, \hat{W}_{i2}, ..., \hat{W}_{in}]^T$ are weights of the NNs with adaptive laws

$$\dot{\hat{W}}_i = -\Gamma_i \left[S_i(Z_i)(v_i - v_{c1i}) + \sigma_i \hat{W}_i \right], \quad i = 1, 2 \quad (58)$$

where $\Gamma = [\Gamma_1, \Gamma_2]^T$ is a positive constant gain matrix and $\sigma = [\sigma_1, \sigma_2]^T$ is a small constant matrix. NNs $\hat{W}^T S(Z)$ are used to approximate $W^{*T} S(Z)$ defined by

$$W^{*T} S(Z) = M_1 \dot{v}_{c0} + \begin{bmatrix} \frac{A_1}{(v_1 - v_{c11})} \\ \frac{A_2}{(v_2 - v_{c12})} \end{bmatrix} \otimes F_1 + \varepsilon_2 \quad (59)$$

where $\varepsilon_2 = [\varepsilon_{21}, \varepsilon_{22}]^T$ is the approximation error. Fig. 1 demonstrates the block diagram of the proposed controller.

B. Stability Analysis of the Adaptive NN Control Law

Theorem 2: For the system described by (1), with the control law (57) and adaptive laws (58), for initial states satisfying the constraints $|v_i| < v_{u1i}, i = 1, 2$, the states of the system would not violate the constraints. When $|v_{c0i}| < v_{u2i}, i = 1, 2$, the closed-loop control system is semiglobally uniformly ultimately bounded; the error signals z and e would converge to compact sets Ω_2 and Ω_3, respectively, where Ω_2 and Ω_3 are defined as

$$\Omega_2 := \{z \in \mathbb{R}^2 | \|z\| \le \sqrt{D}\} \quad (60)$$

$$\Omega_3 := \left\{ e \in \mathbb{R}^3 \Big| \|e\| < \left(\sqrt{\frac{1}{k_1}} \varepsilon_4 + \frac{\varepsilon_3}{2k_1} \right) + 2 \left(\sqrt{\frac{k_2}{k_3}} \varepsilon_4 + \frac{\varepsilon_3}{2k_3} \right) \right.$$
$$\left. + l \left\{ \left(\sqrt{\frac{1}{k_1}} \varepsilon_4 + \frac{\varepsilon_3}{2k_1} \right) + 2 \left(\sqrt{\frac{k_2}{k_3}} \varepsilon_4 + \frac{\varepsilon_3}{2k_3} \right) \right\} \right\}$$
$$(61)$$

where $D = 4 \frac{C_3}{\rho_2}$, $\varepsilon_3 = \sqrt{D}$, $\varepsilon_4 = \frac{\varepsilon_3^2}{4k_1} + \frac{\varepsilon_3^2}{4k_2 k_3}$, l is the minimum value satisfies $l > 5$, $\frac{10}{lk_2 v_{1d\min}} < 0.2$, $\frac{k_3}{2k_2 l^2} < 0.5$, $\frac{k_3}{k_2 v_{1d\min} l} < 0.1$, $1.1 v_{2\max} \frac{10}{lk_2 v_{1d\min}} + v_{1d\max} (\frac{1}{l} + \frac{11 v_{1d\max}}{l v_{1d\min}} + \frac{k_3}{5l}) \frac{10}{lk_2 v_{1d\min}} < 0.2$, and $\frac{k_3}{lk_2 v_{1d\min}} (1 + 1.1 k_2 v_{1d\max} \frac{10}{v_{1d\min}} + \frac{k_3}{5}) < 0.2$. C_3, ρ_2, k_1, k_2, and k_3 are positive constants.

Proof: Considering the following Lyapunov candidate function:

$$V_3 = V_1 + \frac{1}{2} \sum_{i=1}^{2} M_{1ii}^{-1} \Gamma_i^{-1} \tilde{W}_i^T \tilde{W}_i \quad (62)$$

where $\tilde{W}_i = \hat{W}_i - W_i^*$ are weight errors.

Differentiating (62) with respect to time yields

$$\dot{V}_3 = \dot{V}_1 + \sum_{i=1}^{2} M_{1ii}^{-1} \Gamma_i^{-1} \tilde{W}_i^T \dot{\tilde{W}}_i. \quad (63)$$

V_3 can be divided into two parts corresponding to v_1 and v_2, respectively:

$$V_3 = V_{31} + V_{32}. \quad (64)$$

Then, (63) becomes

$$\dot{V}_3 = \dot{V}_{31} + \dot{V}_{32} \quad (65)$$

$$\begin{bmatrix} \dot{V}_{31} \\ \dot{V}_{32} \end{bmatrix} = \begin{bmatrix} \dot{V}_{11} \\ \dot{V}_{12} \end{bmatrix} + \begin{bmatrix} M_{111}^{-1} \Gamma_1^{-1} \tilde{W}_1^T \dot{\tilde{W}}_1 \\ M_{122}^{-1} \Gamma_2^{-1} \tilde{W}_2^T \dot{\tilde{W}}_2 \end{bmatrix} \quad (66)$$

$$= A \otimes \dot{v} - (v - v_{c1}) \otimes \dot{v}_{c0} + M_1^{-1} \begin{bmatrix} \Gamma_1^{-1} \tilde{W}_1^T \dot{\tilde{W}}_1 \\ \Gamma_2^{-1} \tilde{W}_2^T \dot{\tilde{W}}_2 \end{bmatrix}. \quad (67)$$

Substituting (4) and $\tilde{W}_i = \hat{W}_i - W_i^*$ into (67) yields

$$\begin{bmatrix} \dot{V}_{31} \\ \dot{V}_{32} \end{bmatrix} = A \otimes (M_1^{-1}(B_1 \tau - F_1))$$
$$- (v - v_{c1}) \otimes \dot{v}_{c0} + M_1^{-1} \begin{bmatrix} \Gamma_1^{-1} \tilde{W}_1^T \dot{\tilde{W}}_1 \\ \Gamma_2^{-1} \tilde{W}_2^T \dot{\tilde{W}}_2 \end{bmatrix}. \quad (68)$$

Using control law (57) and $\tilde{W}_i = \hat{W}_i - W_i^*$, we have

$$\begin{bmatrix} \dot{V}_{31} \\ \dot{V}_{32} \end{bmatrix} = -\rho_1 M_1^{-1} \begin{bmatrix} V_{11} \\ V_{12} \end{bmatrix} + M_1^{-1} \begin{bmatrix} \Gamma_1^{-1} \tilde{W}_1^T \dot{\hat{W}}_1 \\ \Gamma_2^{-1} \tilde{W}_2^T \dot{\hat{W}}_2 \end{bmatrix}$$
$$+ M_1^{-1} \left\{ (v - v_{c1}) \otimes (W^* + \tilde{W})^T S(Z) \right\}$$
$$- A \otimes (M_1^{-1} F_1) - (v - v_{c1}) \otimes \dot{v}_{c0}. \quad (69)$$

Since M_1^{-1} is a diagonal positive-definite matrix, one has

$$\begin{bmatrix} \dot{V}_{31} \\ \dot{V}_{32} \end{bmatrix} = -\rho_1 M_1^{-1} \begin{bmatrix} V_{11} \\ V_{12} \end{bmatrix} + M_1^{-1} \begin{bmatrix} \Gamma_1^{-1} \tilde{W}_1^T \dot{\hat{W}}_1 \\ \Gamma_2^{-1} \tilde{W}_2^T \dot{\hat{W}}_2 \end{bmatrix}$$
$$+ M_1^{-1} \left\{ (v - v_{c1}) \otimes (\tilde{W}^T S(Z) + \varepsilon_2) \right\}. \quad (70)$$

Substituting (58) into (70) and using $\tilde{W}_i = \hat{W}_i - W_i^*$, we obtain

$$\begin{bmatrix} \dot{V}_{31} \\ \dot{V}_{32} \end{bmatrix} = -\rho_1 M_1^{-1} \begin{bmatrix} V_{11} \\ V_{12} \end{bmatrix} - M_1^{-1} \begin{bmatrix} \sigma_1 \tilde{W}_1^T \hat{W}_1 \\ \sigma_2 \tilde{W}_2^T \hat{W}_2 \end{bmatrix}$$
$$+ M_1^{-1} \left\{ (v - v_{c1}) \otimes \varepsilon_2 \right\} \quad (71)$$

$$\le -\rho_1 M_1^{-1} \begin{bmatrix} V_{11} \\ V_{12} \end{bmatrix} + \frac{1}{2} M_1^{-1} \begin{bmatrix} \|v_1 - v_{c11}\|^2 \\ \|v_2 - v_{c12}\|^2 \end{bmatrix}$$
$$+ \frac{1}{2} M_1^{-1} \begin{bmatrix} \|\bar{\varepsilon}_{21}\|^2 \\ \|\bar{\varepsilon}_{22}\|^2 \end{bmatrix} - M_1^{-1} \begin{bmatrix} \sigma_1 \tilde{W}_1^T (\tilde{W}_1 + W_1^*) \\ \sigma_2 \tilde{W}_2^T (\tilde{W}_2 + W_2^*) \end{bmatrix} \quad (72)$$

$$\le -\rho_1 M_1^{-1} \begin{bmatrix} V_{11} \\ V_{12} \end{bmatrix} + \frac{1}{2} M_1^{-1} \begin{bmatrix} \|v_1 - v_{c11}\|^2 \\ \|v_2 - v_{c12}\|^2 \end{bmatrix}$$

$$-\frac{1}{2}M_1^{-1}\begin{bmatrix}\sigma_1\left\|\tilde{W}_1\right\|^2\\\sigma_2\left\|\tilde{W}_2\right\|^2\end{bmatrix}+\frac{1}{2}M_1^{-1}\begin{bmatrix}\sigma_1\left\|W_1^*\right\|^2\\\sigma_2\left\|W_2^*\right\|^2\end{bmatrix}$$

$$+\frac{1}{2}M_1^{-1}\begin{bmatrix}\left\|\bar{\varepsilon}_{21}\right\|^2\\\left\|\bar{\varepsilon}_{22}\right\|^2\end{bmatrix}. \tag{73}$$

In order to compare V_{1i} and $\frac{1}{2}(v_i - v_{c1i})^2, i = 1, 2$, partially differentiating V_{1i} with respect to v_i, we have

$$\frac{\partial V_{1i}}{\partial v_i} = A_i \tag{74}$$

$$\frac{\partial^2 V_{1i}}{\partial v_i^2} = 1 + \frac{h_i(v_i)}{(v_{u11} - |v_1|)^2} \geq 1. \tag{75}$$

Partially differentiating $\frac{(v_i - v_{c1i})^2}{2}$ with respect to v_i yields

$$\frac{\partial\{\frac{1}{2}(v_i - v_{c1i})^2\}}{\partial v_i} = v_i - v_{c1i} \tag{76}$$

$$\frac{\partial^2\{\frac{1}{2}(v_i - v_{c1i})^2\}}{\partial v_i^2} = 1. \tag{77}$$

For

$$V_{1i}|_{v=v_{c1i}} = \frac{1}{2}(v_i - v_{c1i})^2|_{v=v_{c1i}} = 0 \tag{78}$$

$$\frac{\partial V_{1i}}{\partial v_i}|_{v=v_{c1i}} = \frac{\partial\{\frac{1}{2}(v_i - v_{c1i})^2\}}{\partial v_i} = 0 \tag{79}$$

and

$$\frac{\partial^2 V_{1i}}{\partial v_i^2} \geq \frac{\partial^2\{\frac{1}{2}(v_i - v_{c1i})^2\}}{\partial v_i^2} > 0 \tag{80}$$

we can obtain

$$V_{1i} \geq \frac{1}{2}(v_i - v_{c1i})^2. \tag{81}$$

Then, from (65), (73), and (81), we can obtain

$$\begin{bmatrix}\dot{V}_{31}\\\dot{V}_{32}\end{bmatrix} \leq -(\rho_1 - 1)M_1^{-1}\begin{bmatrix}V_{11}\\V_{12}\end{bmatrix} + \frac{1}{2}M_1^{-1}\begin{bmatrix}\left\|\bar{\varepsilon}_{21}\right\|^2\\\left\|\bar{\varepsilon}_{22}\right\|^2\end{bmatrix} \tag{82}$$

$$-\frac{1}{2}\begin{bmatrix}M_{111}^{-1}\sigma_1\left\|\tilde{W}_1\right\|^2\\M_{122}^{-1}\sigma_2\left\|\tilde{W}_2\right\|^2\end{bmatrix} + \frac{1}{2}\begin{bmatrix}M_{111}^{-1}\sigma_1\left\|W_1^*\right\|^2\\M_{122}^{-1}\sigma_2\left\|W_2^*\right\|^2\end{bmatrix} \tag{83}$$

$$\leq -\rho_2\begin{bmatrix}V_{31}\\V_{32}\end{bmatrix} + \begin{bmatrix}C_1\\C_2\end{bmatrix} \tag{84}$$

and

$$\dot{V}_3 \leq -\rho_2 V_3 + C_3 \tag{85}$$

where

$$\rho_2 = \min\left((\rho_1 - 1)\lambda_{\min}(M_1^{-1}), \min_{i=1,2}(\sigma_i\Gamma_i)\right) \tag{86}$$

$$C_i = \frac{1}{2}M_{1ii}^{-1}\left\|\bar{\varepsilon}_{2i}\right\|^2 + \frac{1}{2}M_{1ii}^{-1}\sigma_i\left\|W_i^*\right\|^2, \quad i = 1, 2 \tag{87}$$
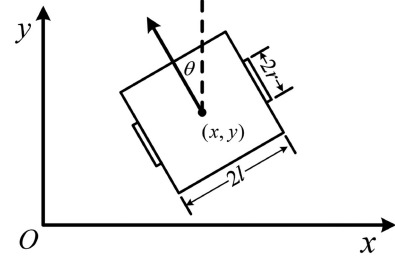
$$C_3 = C_1 + C_2. \tag{88}$$

Fig. 2. Coordinate of the WMR system.

According to the above Lyapunov function, we can conclude that V_3 can converge to an arbitrarily small value by increasing ρ_2. If the auxiliary input velocity v_{c0} is large, or even greater than constraints, i.e., $|v_{c01}| > v_{u11}$ or $|v_{c02}| > v_{u12}$, the proposed method can limit the velocity to satisfy the constraints for safety, which is more important than stable tracking. If $|v_{c0i}| < v_{u2i}, i = 1, 2$, we have $v_{c1} = v_{c0}$ and $\frac{1}{2}(v - v_{c0})^T(v - v_{c0}) < V_3$. For V_3 can converge to be less than arbitrarily small value by increasing ρ_2, we know that z can converge to arbitrarily small values, i.e. for any $\varepsilon_3 > 0$ and initial state $v_i(0) < v_{u2i}, i = 1, 2$, choose $\sqrt{\frac{4C_3}{\rho_2}} = \varepsilon_3$, there exits $T > 0$, when $t > T$ and $|v_{c0i}| < v_{u2i}, i = 1, 2$, we have $\|v - v_{c0}\| < \varepsilon_3$, $z_1 < \varepsilon_3$, and $z_2 < \varepsilon_3$. According to the analysis in model-based control, it can be directly obtained that e will converge to $\Omega_3 := \{e \in \mathbb{R}^3 | \|e\| < (\sqrt{\frac{1}{k_1}\varepsilon_4 + \frac{\varepsilon_3}{2k_1}}) + 2(\sqrt{\frac{k_2}{k_3}\varepsilon_4 + \frac{\varepsilon_3}{2k_3}}) + l\{(\sqrt{\frac{1}{k_1}\varepsilon_4 + \frac{\varepsilon_3}{2k_1}}) + 2(\sqrt{\frac{k_2}{k_3}\varepsilon_4 + \frac{\varepsilon_3}{2k_3}})\}\}$, which can arbitrary be small by suitable choice of k_1, k_2, and k_3. According to [31], the closed-loop control system is semiglobally uniformly ultimately bounded.

V. SIMULATIONS

Considering a two-wheeled mobile robot shown in Fig. 2, simulations are carried out to demonstrate the effectiveness of the proposed method. The desired trajectories are given as $x_d = 2\sin(0.1t)$, $y_d = 2 - 2\cos(0.1t)$, and $\theta_d = 0.1t - \frac{\pi}{2}$ where $t \in [0, t_f]$ and $t_f = 80$ s. $q(0) = [-0.5, -0.5, -0.7]^T$, $\dot{q}(0) = [0, 0, 0]^T$, $r = 100$ mm, $l = 250$ mm, and $M = \text{diag}[m, m, I_p]$. In the beginning, $m = 50$ kg, $I_p = 5.4$ kg·m², and friction coefficient $\mu = 0.08$. The parameter of model-based control is equal to the model. We consider that the control torques of the robot are under external disturbances composed of the Gaussian noise with the power of 0 dBW. In order to better simulate the situation that system parameters change in the process of working, we change the system parameters to $m = 65$ kg, $I_p = 7$ kg·m², and $\mu = 0.15$ at $t > 40$.

Simulation studies for proportional–integral–derivative (PID) control, adaptive SMC [32], model-based control (MB), and adaptive NN control (NN) are carried out in this article. The control parameters are chosen as $k_1 = 10$, $k_2 = 5$, and $k_3 = 4$. For PID control, the parameters are chosen as $K_p = \text{diag}[210, 1.1]$ and $K_d = \text{diag}[0.64, 0.08]$. For SMC, the parameters are the same as those in [32]. For model-based control, the parameters are chosen as $\rho = [15, 57.6]^T$, $v_{u1} = [1, 1.5]^T$,

TABLE I
ISE VALUES OF CONTROL BY PID, SMC, MB, AND NN

	(a) Simulations				(b) Practical Experiments		
t(s)	[0,20)	[20,40)	[40,60)	[60,80)	[0,20)	[20,40)	[40,60)
PID	0.8312	0.0007	0.0063	0.0010	1.6469	0.2072	0.1675
SMC	1.7917	0.0289	0.0011	0.0008	1.4787	0.1235	0.1015
MB	0.7292	0.0005	0.0061	0.0073	1.7376	0.1864	0.1897
NN	0.7126	0.0012	0.0021	0.0014	1.7780	0.0122	0.0062

and $v_{u2} = [0.8, 1.3]^T$. For NN control, the parameters are chosen as $\rho_1 = [1350, 21.6]^T$, $\sigma = [0.0001, 0.0001]^T$, and $\Gamma = [20\,000, 800]^T$. $v_{u1} = [1, 1.5]^T$ and $v_{u2} = [0.8, 1.3]^T$. There are 64 nodes for each $S_i(Z)$ with centers chosen in the area of $[-1, 1] \times [-1, 1] \times [-1, 1] \times [-1, 1] \times [-1, 1] \times [-1, 1]$.

The performance measure information system evaluation (ISE) [33] is

$$J(\text{ISE}) = \sum_{k=1}^{N_s} \|q(k) - q_d(k)\|^2 T_{\text{step}}$$

where $\|q(k) - q_d(k)\| = \sqrt{(q(k) - q_d(k))^T (q(k) - q_d(k))}$, T_{step} denotes step time, and N_s is the length of simulation trail.

The results of simulation are shown in Fig. 3 and Table I(a). Fig. 3(a) shows the trajectory, Fig. 3(b) shows values of Lyapunov functions, Fig. 3(c) and (d) shows the linear velocity and angular velocity, and Fig. 3(e)–(h) shows errors of tracking, where d is the distance between the current position and the desired position. The ISE values of the four control algorithms are reported in Table I(a). From Fig. 3(b), it can be observed that the values of Lyapunov functions are decreasing under the proposed control laws; the change trends of values of Lyapunov functions conform to theoretical analysis. Note that V_3 is unavailable, so in NN control, only V_1 is illustrated. From Fig. 3(e)–(h) and Table I(a), it can be observed that all the four kinds of control schemes can track the desired trajectory under external disturbance; the error signals converge to a small neighborhood of zero. However, from Fig. 3(c) and (d) and Table I, we can observe the following.

1) The PID control cannot limit the velocity, which may cause safety problem. When $t > 40$, the performance of PID control becomes poor because of the change of system parameters.

2) For the adaptive SMC, tracking errors reduce with the learning of parameters. When system parameters change at $t = 40$, the adaptive SMC can guarantee the tracking performance with the learning for new parameters. However, the adaptive SMC cannot limit the velocity; the velocity exceeds the limit at the beginning of the simulation.

3) The model-based control can limit velocities to satisfy the constraints and can track the desired trajectory very well if the parameters are accurate. However, when the parameters of the system change at $t = 40$, the tracking performance reduces greatly.

4) For the NN control, the velocity can also be limited within the constraints. The tracking errors reduce with the learning of NNs. When system parameters change
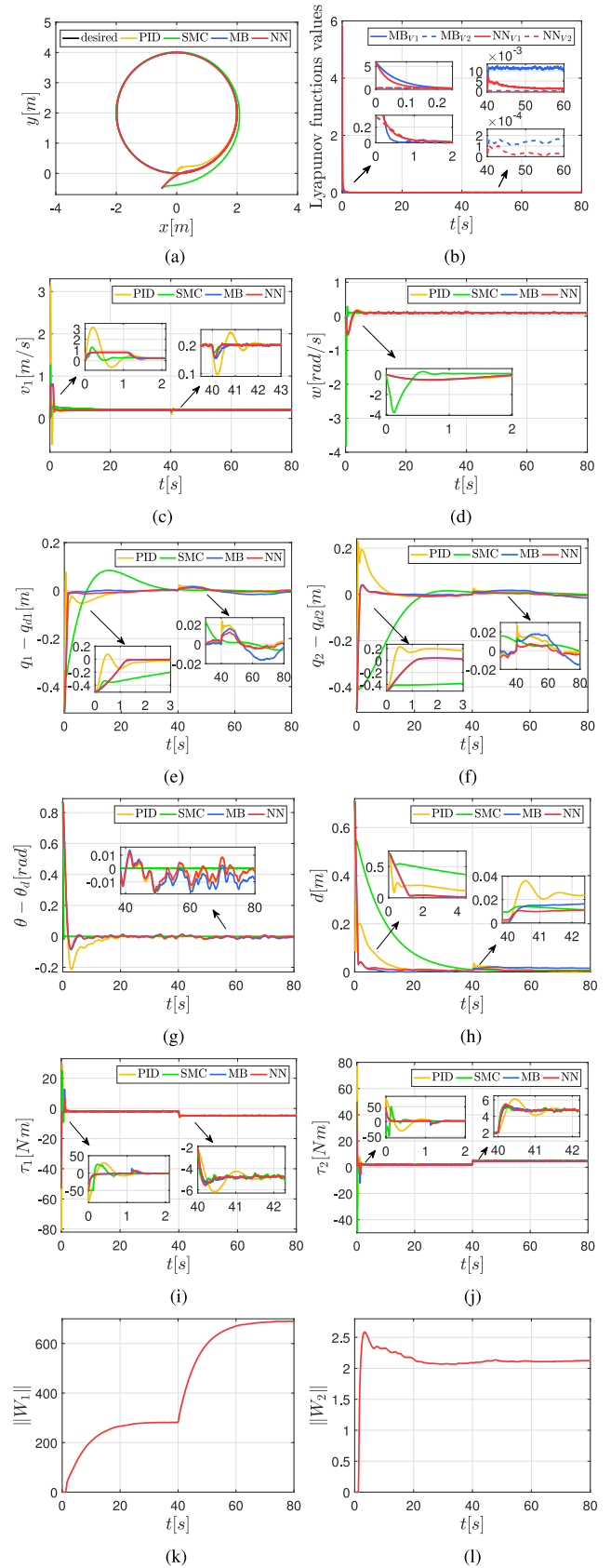

Fig. 3. Simulation results of the closed-loop system. (a) Trajectory. (b) Lyapunov function values. (c) Linear velocity v_1. (d) Angular velocities w. (e) $q_1 - q_{d1}$. (f) $q_2 - q_{d2}$. (g) $\theta - \theta_d$. (h) d. (i) τ_1. (j) τ_2. (k) $\|W_1\|$. (l) $\|W_2\|$.
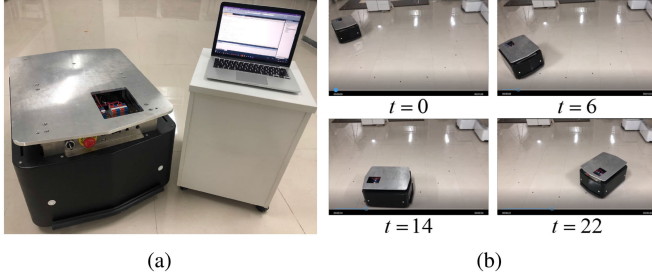
Fig. 4. (a) WMR system. (b) Snapshots of the trajectory tracking.

at $t = 40$, the NNs can learn new parameters, and the tracking performance can be guaranteed.

The input torque of two wheels is given in Fig. 3(i) and (j); it can be observed that the control torque is small enough to be implementable in practice by using motors. The norm of NN weights is given in Fig. 3(k) and (l).

The calculation time of 10 000 times for PID control, adaptive SMC, model-based control, and NN control are 0.4056, 2.0662, 0.3875, and 1.4294 s, respectively, with the MATLAB written simulation program running at a computer equipped with CPU: Intel(R) Core(TM) i5-3210M @2.50 GHz. For all the four kinds of control, the calculation time is short enough that will not affect the tracking performance of the WMR.

VI. PRACTICAL EXPERIMENT

In order to test the performance of the developed control method, a WMR, which is shown in Fig. 4(a), is employed in practical experiments. The WMR has a mass of about 80 kg and a size of 80 cm (length) × 50 cm (width) × 45 cm (height). It is equipped with two driving wheels with servo motors working at torque mode and four passive universal wheels at corners for balance purpose. Driving wheels are mounted in the middle of the WMR's long side. In order to build the map by simultaneous localization and mapping (SLAM), a laser radar with 20-m measurement distance and ±5 cm location error is mounted on the front of the robot. The sampling time of the system is 100 ms.

The results of practical experiment are shown in Figs. 4(b) and Fig. 5 and Table I(b). Fig. 4(b) shows snapshots of the practical experiment. Fig. 5(a) shows the trajectory, Fig. 5(b) shows the values of Lyapunov functions, Fig. 5(c) and (d) shows the linear velocity and the angular velocity, respectively. Fig. 5(e)–(h) shows tracking errors, where d is the distance between the current position and the desired position. The ISE values of the four control algorithms are reported in Table I(b). From Fig. 5(b), it can be observed that the overall trends of values of Lyapunov functions are decreasing under the proposed control laws, which conform to the theoretical analysis. As shown in Fig. 5(a) and (e)–(h), the four kinds of control methods can track the desired trajectory. However, from Fig. 5(c)–(h) and Table I(b), the following can be observed.

1) For the PID control, without constraints for velocity, the position error reduces fastest at the beginning with velocity exceeding the limit; this is dangerous in practice.
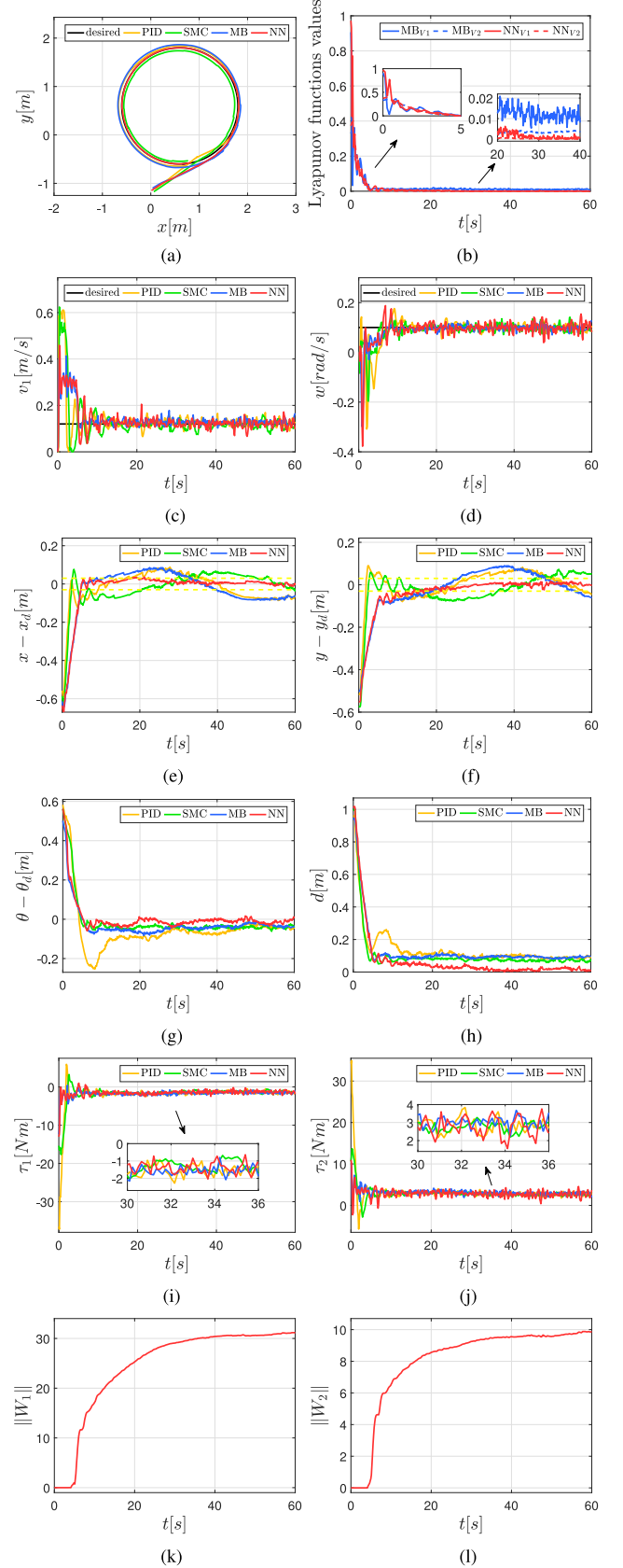2) For the adaptive SMC, with the learning for system parameters, tracking errors converge to small values close

Fig. 5. Experimental results of the closed-loop system. (a) Trajectory. (b) Lyapunov function values. (c) Linear velocity v_1. (d) Angular velocities w. (e) $x - x_d$. (f) $y - y_d$. (g) $\theta - \theta_d$. (h) d. (i) τ_1. (j) τ_2. (k) $\|W_1\|$. (l) $\|W_2\|$.

to zero. However, this method cannot limit the velocity, and the velocity exceeds the limit at the beginning of the experiment.

3) For the model-based control, the velocity is limited to satisfy the constraints. However, system parameters cannot be obtained accurately, so there remain tracking errors greater than NN control.

4) For the NN control, the velocity is also limited within constraints. With the learning of NN weights, tracking errors converge to small values close to zero, and the velocity constraint is guaranteed. The control torque of two wheels is given in Fig. 5(i) and (j). The norm of NN weights is given in Fig. 5(k) and (l).

For the four kinds of control methods, the overshoot of PID control and adaptive SMC is larger than that of both model-based control and NN control. From Fig. 5(c), (d), and (h), it can be observed that PID control and adaptive SMC can eliminate d fast, but they need large velocity, which violates the constraints and may cause harm.

VII. CONCLUSION

In this article, an adaptive NN control scheme was presented for an uncertain nonholonomic WMR with velocity constraints. With the proposed method, the velocity was constrained within the predefined constraints, and the tracking error converged to a small neighborhood of zero. Both simulation studies and practical experiments illustrated that the proposed control can track the desired trajectory with good tracking performance. In the future, we will investigate the problem with finite-time convergence.

REFERENCES

[1] J. X. Xu, Z. Q. Guo, and T. H. Lee, "Design and implementation of integral sliding-mode control on an underactuated two-wheeled mobile robot," *IEEE Trans. Ind. Electron.*, vol. 61, no. 7, pp. 3671–3681, Jul. 2014.

[2] W. He, Y. Dong, and C. Sun, "Adaptive neural impedance control of a robotic manipulator with input saturation," *IEEE Trans. Syst., Man, Cybern., Syst.*, vol. 46, no. 3, pp. 334–344, Mar. 2016.

[3] P. Sun and S. Wang, "Redundant input guaranteed cost non-fragile tracking control for omnidirectional rehabilitative training walker," *Int. J. Control Autom. Syst.*, vol. 13, no. 2, pp. 454–462, 2015.

[4] S. Dong, S. Hu, X. Shao, and L. Chong, "Global stability of a saturated nonlinear PID controller for robot manipulators," *IEEE Trans. Control Syst. Technol.*, vol. 17, no. 4, pp. 892–899, Jul. 2009.

[5] G. Yi, J. Mao, Y. Wang, H. Zhang, and Z. Miao, "Neurodynamics-based leader-follower formation tracking of multiple nonholonomic vehicles," *Assembly Autom.*, vol. 38, no. 5, pp. 548–557, 2018.

[6] C. Hua, C. Lei, Z. Qian, and T. Fei, "Visual servoing of dynamic wheeled mobile robots with anti-interference finite-time controllers," *Assembly Autom.*, vol. 38, no. 5, pp. 558–567, 2018.

[7] M. Velascovilla, E. Arandabricaire, H. Rodriguezcortes, and J. Gonzalezsierra, "Trajectory tracking for a wheeled mobile robot using a vision based positioning system and an attitude observer," *Eur. J. Control*, vol. 18, no. 4, pp. 348–355, 2012.

[8] H. Yang, X. Fan, Y. Xia, and C. Hua, "Robust tracking control for wheeled mobile robot based on extended state observer," *Adv. Robot.*, vol. 30, no. 1, pp. 1–11, 2015.

[9] W. Sun, S. Tang, H. Gao, and J. Zhao, "Two time-scale tracking control of nonholonomic wheeled mobile robots," *IEEE Trans. Control Syst. Technol.*, vol. 24, no. 6, pp. 2059–2069, Nov. 2016.

[10] R. W. Brockett, "Asymptotic stability and feedback stabilization," *Differ. Geometric Control Theory*, vol. 27, pp. 181–191, 1983.

[11] A. M. Bloch, M. Reyhanoglu, and N. H. Mcclamroch, "Control and stabilization of nonholonomic dynamic systems," *IEEE Trans. Autom. Control*, vol. 37, no. 11, pp. 1746–1757, Nov. 1992.

[12] H. Xiao *et al.*, "Robust stabilization of a wheeled mobile robot using model predictive control based on neurodynamics optimization," *IEEE Trans. Ind. Electron.*, vol. 64, no. 1, pp. 505–516, Jan. 2017.

[13] L. Ding, H. Gao, Z. Deng, K. Yoshida, and K. Nagatani, "Slip ratio for lugged wheel of planetary rover in deformable soil: Definition and estimation," in *Proc. IEEE/RSJ Int. Conf. Intell. Robots Syst.*, 2009, pp. 3343–3348.

[14] J. Alvarez-Ramirez, V. Santibanez, and R. Campa, "Stability of robot manipulators under saturated PID compensation," *IEEE Trans. Control Syst. Technol.*, vol. 16, no. 6, pp. 1333–1341, Nov. 2008.

[15] V. Sankaranarayanan and A. D. Mahindrakar, "Configuration constrained stabilization of a wheeled mobile robot theory and experiment," *IEEE Trans. Control Syst. Technol.*, vol. 21, no. 1, pp. 275–280, Jan. 2013.

[16] Y. Zhang, W. Li, and Z. Zhang, "Physical-limits-constrained minimum velocity norm coordinating scheme for wheeled mobile redundant manipulators," *Robotica*, vol. 33, no. 6, pp. 1325–1350, 2015.

[17] C. L. Chen, G. X. Wen, Y. J. Liu, and Z. Liu, "Observer-based adaptive backstepping consensus tracking control for high-order nonlinear semi-strict-feedback multiagent systems," *IEEE Trans. Cybern.*, vol. 46, no. 7, pp. 1591–1601, Jul. 2016.

[18] G. Wen, C. L. P. Chen, Y. J. Liu, and L. Zhi, "Neural network-based adaptive leader-following consensus control for a class of nonlinear multiagent state-delay systems," *IEEE Trans. Cybern.*, vol. 47, no. 8, pp. 2151–2160, Aug. 2017.

[19] W. He and Y. Dong, "Adaptive fuzzy neural network control for a constrained robot using impedance learning," *IEEE Trans. Neural Netw. Learn. Syst.*, vol. 29, no. 4, pp. 1174–1186, Apr. 2018.

[20] S. Zhang, Y. Dong, Y. Ouyang, Z. Yin, and K. Peng, "Adaptive neural control for robotic manipulators with output constraints and uncertainties," *IEEE Trans. Neural Netw. Learn. Syst.*, vol. 29, no. 11, pp. 5554–5564, Nov. 2018.

[21] Y. J. Liu and S. Tong, "Optimal control-based adaptive NN design for a class of nonlinear discrete-time block-triangular systems," *IEEE Trans. Cybern.*, vol. 46, no. 11, pp. 2670–2680, Nov. 2016.

[22] M. Chen and S. S. Ge, "Adaptive neural output feedback control of uncertain nonlinear systems with unknown hysteresis using disturbance observer," *IEEE Trans. Ind. Electron.*, vol. 62, no. 12, pp. 7706–7716, Dec. 2015.

[23] S. Jagannathan and P. He, "Neural-network-based state feedback control of a nonlinear discrete-time system in nonstrict feedback form," *IEEE Trans. Neural Netw.*, vol. 19, no. 12, pp. 2073–2087, Dec. 2008.

[24] J. Chen and H. Qiao, "Muscle-synergies-based neuromuscular control for motion learning and generalization of a musculoskeletal system," *IEEE Trans. Syst., Man, Cybern.: Syst.*, 2020, to be published.

[25] Y. Maeda and M. Iwasaki, "Rheology-based rolling friction modeling with parameterization by neural network," *Seimitsu Kogaku Kaishi/J. Jpn. Soc. Precis. Eng.*, vol. 76, no. 7, pp. 819–826, 2010.

[26] M. L. Corradini, G. Ippoliti, and S. Longhi, "Neural networks based control of mobile robots: Development and experimental validation," *J. Robot. Syst.*, vol. 20, no. 10, pp. 587–600, 2003.

[27] L. Ding, L. Shu, Y. J. Liu, H. Gao, C. Chen, and Z. Deng, "Adaptive neural network-based tracking control for full-state constrained wheeled mobile robotic system," *IEEE Trans. Syst., Man, Cybern.: Syst.*, vol. 47, no. 8, pp. 2410–2419, Aug. 2017.

[28] R. Fierro and F. L. Lewis, "Control of a nonholonomic mobile robot using neural networks," *IEEE Trans. Neural Netw. Learn. Syst.*, vol. 9, no. 4, pp. 589–600, Jul. 1998.

[29] H. Tang and J. Wan, "Robust adaptive control based on neural networks for mobile manipulators," in *Proc. IEEE Int. Conf. Comput. Commun.*, 2017, pp. 947–951.

[30] Y. Kanayama, Y. Kimura, F. Miyazaki, and T. Noguchi, "A stable tracking control method for an autonomous mobile robot," in *Proc. IEEE Int. Conf. Robot. Autom.*, 1991, pp. 384–389.

[31] S. S. Ge, C. C. Hang, T. H. Lee, and T. Zhang, *Stable Adaptive Neural Network Control*, vol. 13. New York, NY, USA: Springer, 2013.

[32] J. Y. Zhai and Z. B. Song, "Adaptive sliding mode trajectory tracking control for wheeled mobile robots," *Int. J. Control*, vol. 92, no. 10, pp. 2255–2262, 2019.

[33] P. Atanu and P. Jagadeesan, "State estimation and nonlinear model based control of a continuous stirred tank reactor using unscented Kalman filter," *Can. J. Chem. Eng.*, vol. 95, no. 7, pp. 1323–1331, 2017.

Ziyu Chen received the B.Eng. degree in automation from the School of Automation, University of Science and Technology Beijing, Beijing, China, in 2016. He is currently working toward the Ph.D. degree in control science and engineering with the University of Science and Technology of China, Hefei, China.

His current research interests include wheeled mobile robotics, neural network control, and robotic control.

Yang Liu received the B.Eng. degree in measurement and control technology and instrumentation program control from the North China University of Water Resources and Electric Power, Zhengzhou, China, in 2013, and the M.Eng. degree in mechanical engineering from the North China University of Technology, Beijing, China, in 2018. He is currently working toward the Ph.D. degree in mechanical engineering with the University of Science and Technology Beijing, Beijing.

His current research interests include robotics, intelligent robot systems, and high-performance robotic manipulation.

Wei He (Senior Member, IEEE) received the B.Eng. degree in automation and the M.Eng. degree in control science and engineering from the College of Automation Science and Engineering, South China University of Technology, Guangzhou, China, in 2006 and 2008, respectively, and the Ph.D. degree in control science and engineering from the Department of Electrical and Computer Engineering, National University of Singapore, Singapore, in 2011.

He is currently a Full Professor with the School of Automation and Electrical Engineering, University of Science and Technology Beijing, Beijing, China. He has coauthored three books published in Springer and authored/coauthored more than 100 international journal and conference papers. His current research interests include robotics, distributed parameter systems, and intelligent control systems.

Dr. He received a Newton Advanced Fellowship from the Royal Society, U.K., in 2017. He was a recipient of the IEEE Systems, Man, and Cybernetics Society Andrew P. Sage Best Transactions Paper Award in 2017. He is the Chair of the IEEE Systems, Man, and Cybernetics Society Beijing Capital Region Chapter. Since 2018, he has been the Chair of the Technical Committee on Autonomous Bionic Robotic Aircraft of the IEEE Systems, Man, and Cybernetics Society. He is an Associate Editor for the IEEE TRANSACTIONS ON ROBOTICS, the IEEE TRANSACTIONS ON NEURAL NETWORKS AND LEARNING SYSTEMS, the IEEE TRANSACTIONS ON SYSTEMS, MAN, AND CYBERNETICS: SYSTEMS, the *Science China Information Sciences*, the IEEE/CAA JOURNAL OF AUTOMATICA SINICA, and *Neurocomputing* and an Editor for the *Journal of Intelligent and Robotic Systems*.

Hong Qiao (Fellow, IEEE) received the B. Eng. degree in hydraulics and control in 1986 and received the M.Eng. degree in robotics and automation in 1989, both from Xi'an Jiaotong University, Xi'an, China, and the Ph.D. degree in robotics control from De Montfort University, Leicester, U.K., in 1995.

She was an Assistant Professor with the City University of Hong Kong and a Lecturer with the University of Manchester from 1997 to 2004. She is currently a Professor with the State Key Laboratory of Management and Control for Complex Systems, Institute of Automation, Chinese Academy of Sciences, Beijing, China. She is also a Professor with the CAS Center for Excellence in Brain Science and Intelligence Technology, Shanghai, China. Her current research interests include robotics, machine learning, and pattern recognition.

Dr. Qiao is a member of the Administrative Committee of the IEEE Robotics and Automation Society. She is the Editor-in-Chief of *Assembly Automation* and an Associate Editor for the IEEE TRANSACTIONS ON CYBERNETICS, the IEEE TRANSACTIONS ON AUTOMATION AND SCIENCES TECHNOLOGY, and the IEEE/ASME TRANSACTIONS ON MECHATRONICS.

Haibo Ji received the B.Eng. degree from Zhejiang University, Hangzhou, China, in 1984, and the Ph.D. degree from Beijing University, Beijing, China, in 1990, both in mechanical engineering.

He is currently a Professor with the Department of Automation, University of Science and Technology of China, Hefei, China. His research interests include nonlinear control and adaptive control.